



## A coarse space for heterogeneous Helmholtz problems based on the Dirichlet-to-Neumann operator



Lea Conen<sup>a,\*</sup>, Victorita Dolean<sup>b,c</sup>, Rolf Krause<sup>a</sup>, Frédéric Nataf<sup>d</sup>

<sup>a</sup> Università della Svizzera italiana, Institute of Computational Science, Via G. Buffi 13, 6900 Lugano, Switzerland

<sup>b</sup> Université de Nice-Sophia Antipolis, Laboratoire J.-A. Dieudonné, CNRS UMR 7351, Parc Valrose, 060108 Nice Cedex 2, France

<sup>c</sup> University of Strathclyde, Dept. of Mathematics and Statistics, 26 Richmond Street, Glasgow G1 1XH, Scotland, UK

<sup>d</sup> Université P. & M. Curie, Laboratoire J.L. Lions, CNRS and INRIA Alpines Team, 4 place Jussieu, 75005, Paris, France

### ARTICLE INFO

#### Article history:

Received 11 June 2013

Received in revised form 17 February 2014

#### Keywords:

Helmholtz equation

Domain decomposition

Coarse space

Dirichlet-to-Neumann operator

### ABSTRACT

The Helmholtz equation governing wave propagation and scattering phenomena is difficult to solve numerically. Its discretization with piecewise linear finite elements results in typically large linear systems of equations. The inherently parallel domain decomposition methods constitute hence a promising class of preconditioners. An essential element of these methods is a good coarse space. Here, the Helmholtz equation presents a particular challenge, as even slight deviations from the optimal choice can be devastating.

In this paper, we present a coarse space that is based on local eigenproblems involving the Dirichlet-to-Neumann operator. Our construction is completely automatic, ensuring good convergence rates without the need for parameter tuning. Moreover, it naturally respects local variations in the wave number and is hence suited also for heterogeneous Helmholtz problems. The resulting method is parallel by design and its efficiency is demonstrated on 2D homogeneous and heterogeneous numerical examples.

© 2014 Elsevier B.V. All rights reserved.

## 1. Introduction

The Helmholtz equation

$$-\Delta u - k^2 u = f \tag{1}$$

with suitable boundary conditions and wave number  $k > 0$  governs wave propagation and scattering phenomena arising in a wide range of engineering applications, such as aeronautics, underwater acoustics, and geophysical seismic imaging. Its discretization with piecewise linear finite elements results for large wave number  $k$  in an indefinite, ill-conditioned linear system of equations. Indefiniteness could be avoided using a non-standard variational formulation [1]. The number of grid points grows rapidly with  $k$  in order to maintain accuracy and to avoid the pollution effect [2]. As the linear system of equations is hard to solve for iterative methods [3,4], carefully designed methods are necessary.

There has been a vast amount of research on this topic, including incomplete factorization methods [5–8] and the “sweeping preconditioner” [9]. Preconditioning with a shifted, easier problem has been considered e.g. in [10,11]. The problems encountered when multigrid methods are applied to the Helmholtz equation have been analyzed in detail [12,13]. Particularly interesting is the wave-ray multigrid [12], where special levels based on plane waves that lie in the kernel of the homogeneous, continuous Helmholtz operator are introduced, designed to represent the oscillatory part of the solution.

\* Corresponding author. Tel.: +41 0 58 666 4975.

E-mail addresses: [lea.conen@usi.ch](mailto:lea.conen@usi.ch) (L. Conen), [dolean@unice.fr](mailto:dolean@unice.fr) (V. Dolean), [rolf.krause@usi.ch](mailto:rolf.krause@usi.ch) (R. Krause), [nataf@ann.jussieu.fr](mailto:nataf@ann.jussieu.fr) (F. Nataf).

In this work, we concentrate on domain decomposition methods (DDMs), see e.g. [14]. As the systems of linear equations resulting from the discretization of Problem (1) are typically large, these methods constitute due to their inherent parallelism an interesting class of preconditioners. DDMs have two main ingredients: the transmission conditions, specifying the information exchange between neighboring subdomains and the coarse space, allowing for global transfer of information. Unfortunately, classical choices for either of these two parts are not effective for the Helmholtz equation. This led to the development of specially adapted methods, see [15] for a numerical comparison.

Early work on transmission conditions for the Helmholtz equation was done in [16], where a first order approximation to the Sommerfeld radiation condition is employed. In the sequel, different, more advanced techniques have been used; including PML at the interfaces [17–19], non-local transmission conditions [20], optimized Schwarz methods [21], and others, e.g. [22].

Originally used in the multigrid context [12], plane waves have been successfully employed also as coarse space basis functions for DDMs. Their evaluation at the subdomains' interfaces are used in the FETI(-DP)-H methods [23,24]. Later, they have also been used in other DDMs [25,26] and as deflation vectors [27]. Plane waves, to our knowledge, have been employed mainly for homogeneous problems; the extension to heterogeneous ones is not obvious.

In this paper, we concentrate on the development of a coarse space for a restricted additive Schwarz method. We adapt an idea for elliptic problems where the coarse space is based on local functions, the solutions of eigenproblems involving the Dirichlet-to-Neumann operator on the subdomains' interfaces [28,29]. Our coarse space is robust with respect to heterogeneous coefficients and its construction is completely automatic, refraining from the need for parameter tuning. The latter feature is crucial for indefinite problems as in contrast to the elliptic case, even slight deviations from the optimal choice can be fatal [30].

The paper is organized as follows. The Helmholtz equation is introduced in Section 2, the two-level DDM in Section 3. In Section 4, we motivate and define our coarse space. Emphasis is put on the development of a criterion for choosing the coarse space size automatically. Section 5 elaborates on the effect the second level has on spectrum and convergence rates. In Section 6, we test the DtN coarse space numerically and compare it to the standard one based on plane waves.

## 2. Helmholtz equation and discretization

We are interested in the interior Helmholtz problem of the following form: let  $\Omega \subset \mathbb{R}^d$ ,  $d = 2, 3$ , be a polygonal, bounded domain. Find  $u : \Omega \rightarrow \mathbb{C}$  s.t.

$$-\Delta u - k^2 u = f \quad \text{in } \Omega, \quad (2a)$$

$$u = 0 \quad \text{on } \Gamma_D, \quad (2b)$$

$$\frac{\partial u}{\partial n} + iku = 0 \quad \text{on } \Gamma_R, \quad (2c)$$

where  $\Gamma_D \cup \Gamma_R = \Gamma := \partial\Omega$  is a disjoint partition of  $\partial\Omega$ . We abbreviate the boundary conditions in the form  $\mathcal{C}(u) = 0$  on  $\Gamma$ . The wave number  $k$  is given by  $k(\vec{x}) = \omega/c(\vec{x})$ , where  $\omega$  is the angular frequency and  $c$  is the speed of propagation that might depend on  $\vec{x} \in \Omega$ . Eq. (2c) is designed to approximate an unbounded domain and is a first order approximation of the Sommerfeld radiation condition, c.f. [31].

Denoting by  $H^1(\Omega)$  the usual Sobolev space of order 1 on  $\Omega$ , the variational formulation of Problem (2) is: find  $u \in V := \{u \in H^1(\Omega) : u = 0 \text{ on } \Gamma_D\}$  s.t.

$$a(u, v) = F(v) \quad \forall v \in V, \quad (3)$$

where  $a(\cdot, \cdot) : V \times V \rightarrow \mathbb{C}$  and  $F : V \rightarrow \mathbb{C}$  are defined by

$$a(u, v) = \int_{\Omega} (\nabla u \nabla v - k^2 uv) \, dx + \int_{\Gamma_R} iku v \, ds, \quad F(v) = \int_{\Omega} f v \, dx.$$

It is well-posed if  $\Gamma_R \neq \emptyset$ , c.f. [32, Chapter 2]. We consider a discretization of the variational problem (3) using piecewise linear finite elements on a uniform triangular mesh  $\mathcal{T}_h$  of  $\Omega$ . Denoting by  $V_h \subset V$  the corresponding finite element space, it reads: find  $u_h \in V_h$  such that

$$a(u_h, v_h) = F(v_h) \quad \forall v_h \in V_h. \quad (4)$$

With  $\{\phi_k\}_{k=1}^n$  the nodal linear finite element basis for  $V_h$ ,  $n := \dim(V_h)$ , we rewrite (4) in matrix form:

$$A\vec{u} = \vec{f}, \quad (5)$$

where the coefficients of the stiffness matrix  $A \in \mathbb{C}^{n \times n}$  and the right-hand side  $\vec{f} \in \mathbb{C}^n$  are given by  $A_{k,l} = a(\phi_l, \phi_k)$  and  $\vec{f}_k = F(\phi_k)$ . The resulting matrix is indefinite and without the Sommerfeld boundary condition possibly singular. It is complex symmetric when  $\Gamma_R \neq \emptyset$ .

## 3. Two-level restricted additive Schwarz method

This section defines the domain decomposition method (DDM) that we use as a preconditioner for the Helmholtz equation (5). It is a two-level restricted additive Schwarz (RAS) method [14] with suitable transmission conditions.

We partition the domain  $\Omega$  into a set of non-overlapping subdomains  $\{\Omega_j'\}_{j=1}^N$  resolved by the mesh  $\mathcal{T}_h$ . The overlapping subdomains  $\Omega_j$  are then defined by adding one or several layers of mesh elements to  $\Omega_j'$  in the following sense:

**Definition 3.1.** Given a subdomain  $D' \subset \Omega$ , which is resolved by the finite element mesh  $\mathcal{T}_h$ , the extension  $D$  of  $D'$  by one layer of elements is

$$D = \text{Int} \left( \bigcup_{\text{supp}(\phi_k) \cap D' \neq \emptyset} \text{supp}(\phi_k) \right),$$

where  $\text{Int}(\cdot)$  denotes the interior of a domain. Extensions by more than one layer are defined recursively.

This gives an overlapping partition  $\{\Omega_j\}$  of  $\Omega$ . Let  $V_h(\Omega_j) = \{v|_{\Omega_j} : v \in V_h\}$ ,  $1 \leq j \leq N$ , denote the space of functions in  $V_h$  restricted to the subdomain  $\Omega_j$ . Let  $n := |\text{dof}(\Omega)|$  and  $n_j := |\text{dof}(\Omega_j)|$ ,  $1 \leq j \leq N$ , where for  $D \subseteq \Omega$  we define  $\text{dof}(D) := \{k : \text{supp}(\phi_k) \subset \bar{D}\}$ .

For  $1 \leq j \leq N$ , we define a restriction operator  $\mathcal{R}_j : V_h \rightarrow V_h(\Omega_j)$ : for  $u \in V_h$ , we set  $(\mathcal{R}_j u)(\vec{x}_i) = u(\vec{x}_i)$  for all  $\vec{x}_i \in \Omega_j$ . We denote the corresponding matrix in  $\mathbb{R}^{n_j \times n}$  that maps coefficient vectors of functions in  $V_h$  to coefficient vectors of functions in  $V_h(\Omega_j)$  by  $R_j$ . Let  $D_j \in \mathbb{R}^{n_j \times n_j}$  be a diagonal matrix corresponding to a partition of unity in the sense that  $\sum_{i=1}^N \tilde{R}_i^T R_i = I$ , where  $\tilde{R}_j := D_j R_j$ . Then the RAS preconditioner reads

$$M^{-1} := \sum_{j=1}^N \tilde{R}_j^T A_j^{-1} R_j. \quad (6)$$

It remains to define the subdomain matrices  $A_j$ . With the classical choice  $A_j = R_j A R_j^T$ , frequencies in the error smaller than the wave number  $k$  are not damped [21]. This might cause slow convergence or even stagnation of the iterative method. Therefore, we define the matrices  $A_j$  in (6) to be the stiffness matrices of the local Robin problems [16,33]

$$\begin{aligned} (-\Delta - k^2)(u_j) &= f \quad \text{in } \Omega_j, \\ \mathcal{C}(u_j) &= 0 \quad \text{on } \partial\Omega \cap \partial\Omega_j, \\ \left(\frac{\partial}{\partial n_j} + ik\right)(u_j) &= 0 \quad \text{on } \partial\Omega_j \setminus \partial\Omega. \end{aligned}$$

More advanced techniques such as optimized boundary conditions [34] are also possible, but not considered here.

DDMs as above do not show convergence rates independent of the number of subdomains [14]. In order to achieve independence, one possibility is to add a coarse space to the iteration procedure (6) via the balancing Neumann–Neumann (BNN) method [35]. For non-symmetric systems, it reads [36]:

$$P_{\text{BNN}} = QM^{-1}P + ZE^{-1}Y^\dagger, \quad (7)$$

where  $\dagger$  denotes the conjugate transpose,  $M^{-1}$  is the one-level preconditioner (6),  $Z$  and  $Y$  are rectangular matrices with full column rank,  $E = Y^\dagger A Z$  is the coarse grid matrix,  $\mathcal{E} = ZE^{-1}Y^\dagger$  is the coarse grid correction matrix, and  $P = I - A\mathcal{E}$  and  $Q = I - \mathcal{E}A$  are projection matrices. We only consider the case  $Z = Y$  and will define  $Z$  in Section 4.

Following this notation,  $Z$  implicitly defines what is called the coarse space  $W$ , i.e. the columns of  $Z$  represent the basis vectors of  $W$ . The choice of  $Z$ , and hence of the coarse space  $W$  itself, influences the convergence speed of the resulting two-level method (7) significantly. For indefinite systems, the correctness of the coarse space is especially important, as, contrarily to the elliptic case, any deviation from the optimal setting might be fatal, c.f. Section 5.1 and [30]. Hence particular emphasis has to be put on the design of  $W$ .

#### 4. Dirichlet-to-Neumann coarse space for the Helmholtz equation

Whereas for certain elliptic problems choices of the coarse space  $W$  are known that turn one-level DDMs into optimal solvers with subdomain independent convergence rates [14], for the Helmholtz problem the situation is much more complicated. Various approaches can be found in the literature that aim at designing efficient two-level methods [12,23–27], often using plane waves as basis functions for the coarse space. Although very elegant by design, this construction does not cover the case of varying coefficients and requires an a priori choice of certain parameters. Here, we therefore aim at constructing a coarse space with the following properties: on the one hand, for constant coefficients it behaves similarly as the one based on plane waves. On the other hand, it is also efficient for heterogeneous coefficients and can be constructed in an automatic, parameter-free fashion. The construction is based on local eigenproblems involving the Dirichlet-to-Neumann operator (DtN), c.f. [29].

##### 4.1. What should the coarse space look like?

*The subdomain structure should be reflected in the coarse space.* The Richardson iteration (without relaxation) for the system preconditioned with  $M^{-1}$  reads  $\vec{r}^{k+1} = (I - M^{-1}A) \vec{r}^k$ , where  $\vec{r}^k = \vec{f} - A\vec{x}^k$  is the residual. The one-level RAS preconditioner

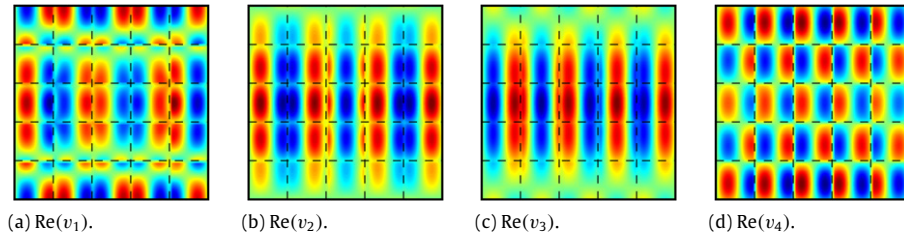


**Fig. 1.** Real part of optimal coarse space function  $v_i$  associated to eigenvalue  $\lambda_i$ ,  $|\lambda_i| \geq |\lambda_{i+1}|$  for all  $i$ , of (8) on  $\Omega$ ,  $5 \times 5$  subdomains,  $n_{\text{loc}} = 40$ ,  $k = 29.3$ .

$M^{-1}$  is consequently not efficient for eigenfunctions associated to eigenvalues with large modulus of  $I - M^{-1}A$ . These are the functions that should enter the coarse space. To compute these “optimal” coarse space functions, we hence solve the eigenproblem

$$\text{Find } (v_i, \lambda_i) \in \mathbb{C}^n \times \mathbb{C}, \quad 1 \leq i \leq n, \text{ such that } (I - M^{-1}A)v_i = \lambda_i v_i, \quad (8)$$

and then choose those functions  $v_i$  for which the modulus of the associated eigenvalue  $|\lambda_i|$  is large. The structure of the resulting functions  $v_i$  in Fig. 1 clearly reflects the domain partition, suggesting a subdomain based construction.

*In the interior of each subdomain, the homogeneous problem should be solved.* One can check numerically that the optimal coarse functions solve the local problems with zero right-hand side in the interior of each subdomain away from the overlap. Moreover, it is easy to see that the RAS iterates solve the Helmholtz equation inside each subdomain. A coarse space correction that solves the homogeneous equation inside each subdomain conserves this property and does not introduce additional errors.

*Eigenfunctions on the interface are well-suited to capture varying coefficients.* As local problems are solved exactly, all the work is done on the interface/in the overlap. Therefore, also the eigenproblems should be posed in that region. This has been proven true in a number of works, considering however definite problems, see e.g. [28,29,37].

*Frequencies close to the wave number  $k$  are not handled well by the one-level method.* Fourier analysis for a two subdomain model problem shows that Fourier frequencies close to the wave number  $k$  have the worst convergence rates, c.f. [38]. Varying the wave number for the eigenproblem (8), in Fig. 2 we see that also in our setting of overlapping subdomains, which is different from the one used for the Fourier analysis, in the direction orthogonal to the Dirichlet boundary conditions the worst eigenfunctions clearly depend on the wave number.

#### 4.2. Definition of the coarse space based on the Dirichlet-to-Neumann operator

In this section, we introduce our coarse space for the Helmholtz equation. It is based on eigenproblems involving local DtN maps and incorporates naturally the possible heterogeneity in the wave number. The underlying idea originates from work on elliptic problems [28,29,37]. This construction respects the main principles outlined in Section 4.1: apart from including all the important modes, in the interior of each subdomain the coarse functions lie in the kernel of the Helmholtz operator and the construction is based on local problems only. The latter makes it possible to construct the coarse space efficiently in parallel.

The coarse space functions are local functions that are eigenfunctions of the DtN operator on the boundary of a subdomain. We first consider the continuous formulation of the DtN eigenproblems. On each interface  $\Gamma_i := \partial\Omega_i \setminus \partial\Omega$  we solve the eigenproblem: find  $(u_{\Gamma_i}, \lambda) \in V(\Gamma_i) \times \mathbb{C}$  such that

$$\text{DtN}_{\Omega_i}(u_{\Gamma_i}) = \lambda u_{\Gamma_i}. \quad (9)$$

For the definition of the DtN operator, we need to extend a function from the boundary of a subdomain to its interior:

**Definition 4.1 (Helmholtz Extension).** Let  $D \subset \Omega$ , let  $\Gamma_D = \partial D \setminus \partial\Omega$ . Let  $v_{\Gamma_D} : \Gamma_D \rightarrow \mathbb{C}$ . The extension  $u : D \rightarrow \mathbb{C}$  of  $v_{\Gamma_D}$  with respect to the Helmholtz operator is defined by

$$\begin{aligned} -\Delta u - k^2 u &= 0 \quad \text{in } D, \\ \mathcal{C}(u) &= 0 \quad \text{on } \partial\Omega \cap \partial D, \\ u &= v_{\Gamma_D} \quad \text{on } \Gamma_D. \end{aligned}$$

The DtN operator is then defined as follows:

**Definition 4.2 (Dirichlet-to-Neumann Operator).** Let  $D \subset \Omega$ , let  $\Gamma_D = \partial D \setminus \partial\Omega$ . Let  $v_{\Gamma_D} : \Gamma_D \rightarrow \mathbb{C}$ . Then

$$\text{DtN}_D(v_{\Gamma_D}) = \frac{\partial u}{\partial n} \Big|_{\Gamma_D},$$

where  $u : D \rightarrow \mathbb{C}$  is the extension of  $v_{\Gamma_D}$  in the sense of Definition 4.1.

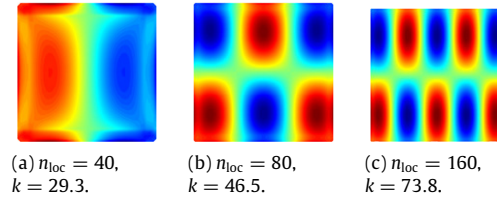


Fig. 2. Real part of optimal coarse space function associated to largest eigenvalue of (8) on central subdomain in a  $5 \times 5$  subdomain decomposition.

We choose  $m_i \in \mathbb{N}$  eigenfunctions for each subdomain  $\Omega_i$  according to the following criterion:

**Criterion 4.3** (*Choice of DtN Eigenfunctions*). On each subdomain  $\Omega_i$ , we choose all eigenfunctions  $v$  of the DtN eigenproblem (9), for which the associated eigenvalue  $\lambda$  satisfies

$$\operatorname{Re}(\lambda) < k_i.$$

Here  $k_i := \max_{\bar{x} \in \Omega_i} k(\bar{x})$  is the maximum wave number on  $\Omega_i$ . If no eigenvalue satisfies this condition, the eigenvalue with smallest real part is chosen.

This criterion provides a way to automatically construct the coarse space  $W$  without the need to tune its dimension, a crucial parameter for the convergence of the two-level method. Numerical evidence that supports Criterion 4.3 is provided in Section 4.3.

We proceed with the discrete formulation of the DtN eigenproblem and explain how to construct the matrix  $Z \in \mathbb{C}^{n \times \sum_{j=1}^N m_j}$  spanning the coarse space. The columns  $1 + \sum_{j=1}^{i-1} m_j, \dots, \sum_{j=1}^i m_j$  of  $Z$  are set to  $R_i^T W_i$  for  $1 \leq i \leq N$ . Here  $W_i \in \mathbb{C}^{n_i \times m_i}$  is a rectangular matrix associated to subdomain  $\Omega_i$ , which is given by Algorithm 4.1.  $Z$  is a rectangular, block-diagonal matrix with blocks  $W_i$  that may have overlapping rows due to the overlap in the domain decomposition. We now define the single components of Algorithm 4.1.

---

**Algorithm 4.1** Construction of the block  $W_i$  of the DtN coarse matrix.

---

- 1: Solve the discrete DtN eigenproblem (10) on subdomain  $\Omega_i$ .
  - 2: Choose  $m_i$  eigenvectors  $\vec{g}_i^k \in \mathbb{C}^{n_{\Gamma_i}}$ ,  $1 \leq k \leq m_i$  by the discrete analogue of Criterion 4.3.
  - 3: **for**  $k \leftarrow 1$  to  $m_i$  **do**
  - 4:   Compute the extension  $\vec{u}_i^k \in \mathbb{C}^{n_i}$  of  $\vec{g}_i^k$  according to Definition 4.4.
  - 5: **end for**
  - 6: Define the matrix  $W_i \in \mathbb{C}^{n_i \times m_i}$  as  $W_i := (D_i \vec{u}_i^1, \dots, D_i \vec{u}_i^{m_i})$ , where  $D_i$  are the matrices corresponding to a partition of unity defined in Section 3.
- 

For Line 1 of Algorithm 4.1, we need the discrete formulation of the DtN eigenproblem (9): let  $I$  and  $\Gamma_i$  be the sets of indices corresponding to the interior and boundary degrees of freedom, respectively. Let  $n_I$  and  $n_{\Gamma_i}$  be their cardinalities. We define  $a_i : H^1(\Omega_i) \times H^1(\Omega_i) \rightarrow \mathbb{R}$ ,

$$a_i(v, w) = \int_{\Omega_i} (\nabla v \cdot \nabla w - k^2 v w) \, dx.$$

Using the finite element basis  $\{\phi_k\}$  for  $V(\Omega)$ , let  $A^{(i)}$  be the coefficient matrix of a Neumann boundary value problem on  $\Omega_i$ ,  $A_{kl}^{(i)} = a_i(\phi_k, \phi_l)$ , with boundary conditions defined by  $\mathcal{C}$  on  $\partial\Omega_i \cap \partial\Omega$ . With the usual block notation, the subscripts  $I$  and  $\Gamma_i$  for the matrices  $A$  and  $A^{(i)}$  denote the entries of these matrices associated to the respective degrees of freedom. Let

$$M_{\Gamma_i} = \left( \int_{\Gamma_i} \phi_k \phi_l \, ds \right)_{k, l \in \Gamma_i}$$

be the mass matrix on the interface of subdomain  $\Omega_i$ . The discrete formulation of the eigenproblem (9) is [28]: For  $1 \leq i \leq N$  find  $(\vec{u}, \lambda) \in \mathbb{C}^{n_{\Gamma_i}} \times \mathbb{C}$ , s.t.

$$\left( A_{\Gamma_i \Gamma_i}^{(i)} - A_{\Gamma_i I} A_{II}^{-1} A_{I \Gamma_i} \right) \vec{u} = \lambda M_{\Gamma_i} \vec{u}. \quad (10)$$

Now we define the extension operator required in Line 4 of Algorithm 4.1:

**Definition 4.4** (*Discrete Helmholtz Extension*). The extension of a vector  $\vec{g} \in \mathbb{C}^{n_{\Gamma_i}}$  defined on the interface  $\Gamma_i$  to all degrees of freedom on subdomain  $\Omega_i$  is the vector  $\vec{u} \in \mathbb{C}^{n_i}$  given by  $\vec{u} = (-A_{II}^{-1} A_{I \Gamma_i} \vec{g}, \vec{g})^T$ .

**Remark 4.5** (*Singular Extension*). The extensions in Definitions 4.1 and 4.4 might give a (numerically) singular problem for subdomains that do not touch the Robin boundary. As those problems are small and are solved directly, strategies for singular systems such as QR decomposition can be employed.

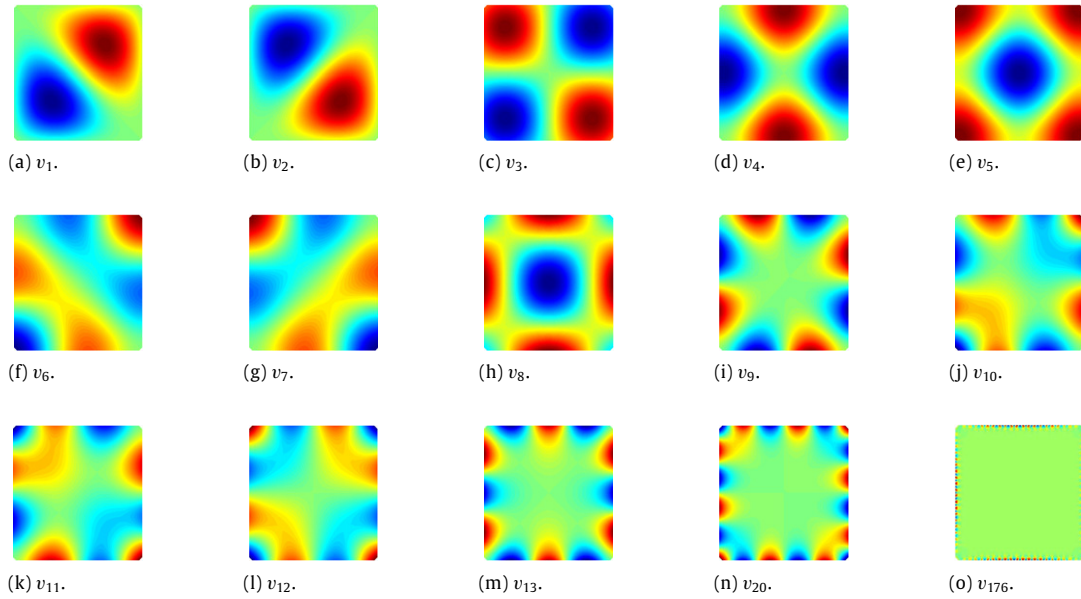


**Fig. 3.** Some DtN eigenfunctions.  $5 \times 5$  subdomains,  $n_{\text{loc}} = 40$ ,  $k = 30$ .

**Table 1**

Iteration numbers for different choices of DtN eigenfunctions.

Choice	# Iterations	
	$m_i = 12$	$m_i = 24$
No coarse space	115	115
$\text{Re}(\lambda)$ minimal	16	10
$ \lambda $ minimal	37	26
$ \lambda - k $ minimal	77	35
$ \lambda $ maximal	115	115

#### 4.3. How to choose the Dirichlet-to-Neumann coarse space functions

For indefinite systems as those arising from the Helmholtz equation, in contrast to the symmetric positive definite case, increasing the dimension of the coarse space might lead to a deterioration of the convergence rates, c.f. Section 5.1 and [30]. An incorrect coarse space might hence be fatal, but it is difficult to decide *a priori* which and how many modes are needed. Thus an appropriate strategy for the coarse space construction is extremely important. In this section, we justify and investigate the coarse space based on the DtN operator introduced in Section 4.2 in detail and test Criterion 4.3.

For the tests, we take the setup described in Section 6.1 and Problem 1 from Section 6.2. Let the domain  $\Omega$  be decomposed into  $5 \times 5$  subdomains,  $n_{\text{loc}} = 40$ ,  $k = 30$ . All experiments in this section are based on this example for the ease of presentation. The conclusions have however also been verified in modified setups. Moreover, they are supported by the numerical experiments in Section 6.

We first examine *which* eigenfunctions of the DtN eigenproblem (10) are important. The eigenvalues  $\lambda_i$ ,  $1 \leq i \leq 176$ ,  $\text{Re}(\lambda_i) \leq \text{Re}(\lambda_{i+1}) \forall i$ , on the central subdomain satisfy  $\text{Re}(\lambda_5) < 0 < \text{Re}(\lambda_6)$ , and  $\text{Re}(\lambda_{12}) < k < \text{Re}(\lambda_{13})$ . We show a few of the extensions to the interior of the subdomains of the associated eigenvectors  $v_i$  in Fig. 3. From this, our first guess is that eigenfunctions associated to smaller eigenvalues are more useful. We check this numerically by comparing coarse spaces with 12 modes per subdomain based on the eigenvalues with the smallest real part, the smallest eigenvalues in modulus, the eigenvalues closest to the wave number  $k = 30$ , and the eigenvalues with the largest modulus. This yields the results in the central columns of Table 1. The first alternative, which is in accordance with Criterion 4.3, gives the best results.

To ensure that our findings are not distorted by choosing a too small coarse space, in the last column of Table 1 the results for the same experiment with a twice as large coarse space are reported. The best strategy seems robust in terms of the number of iterations; it hardly changes compared to the case with smaller coarse space. Also in this setting, Criterion 4.3 performs best.

In the next step, we examine *how many* modes should be chosen. The more important part of this problem is that we should not choose too few modes as the convergence rates cannot be expected to depend monotonically on the coarse space size due to the indefiniteness of the system. Nevertheless, choosing too many modes increases the computational costs and is not desirable either. The number of modes is controlled by Criterion 4.3. In Fig. 4 we show the resulting number of modes per subdomain for a heterogeneous example. They are influenced both by the boundary conditions and the heterogeneity.



		Robin						
Dirichlet		5	8	8	8	5		
		6	9	9	9	6		
		5	8	8	8	5		
		7	11	11	11	7		
		1	1	1	1	1		
		Robin						

**Fig. 4.** Number of DtN modes per subdomain. Heterogeneous Problem 1,  $5 \times 5$  subdomains,  $n_{\text{loc}} = 40$ ,  $k = 30$ .

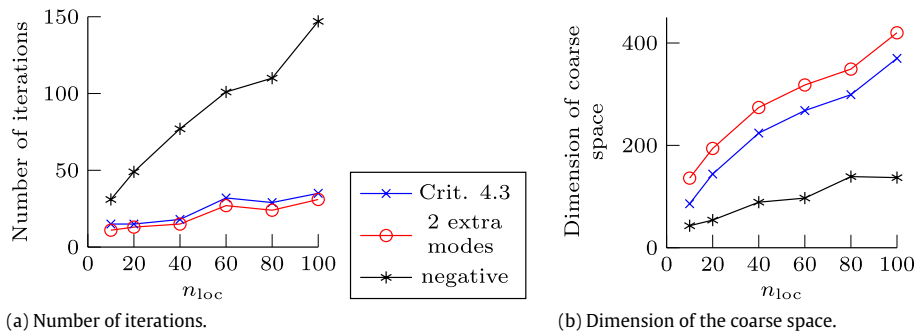


**Fig. 5.** Comparison of different criteria of how many DtN modes to choose.  $k^3 h^2 \approx \frac{2\pi}{10}$ , Problem 1,  $5 \times 5$  subdomains.

**Table 2**

Dependence of the number of iterations with DtN coarse space and the dimension of the DtN coarse space on the size  $L$  of the domain  $\Omega = [0, L]^2$ .  $\Omega$  is decomposed into  $5 \times 5$  subdomains with  $n_{\text{loc}} = 40$  grid points on each subdomain in each direction. The wave number  $k$  is chosen such that  $kL$  is constant.

$L$	$k$	$kL$	# Iterations	Coarse space dimension
1	30	30	24	224
5	6	30	24	224
10	3	30	24	224

In Fig. 5, we examine whether the number of modes resulting from Criterion 4.3 is sensible. It yields convergence rates that are almost independent of grid width/wave number at the cost of an increasing coarse space size. We investigate whether we can do significantly better by adding the next two eigenvectors on each subdomain – where the eigenvalues are ordered by their real parts – to the coarse space. Fig. 5(a) shows that this is not the case, it only yields a slight improvement. Moreover, we test whether we could achieve the same behavior with a significantly smaller coarse space. Therefore, we choose another “natural” bound, taking only eigenvectors that are associated to eigenvalues with real part smaller than 0, denoted by “negative” in the legends. For this choice, the number of iterations significantly increases with  $n_{\text{loc}}$  and hence with  $k$ .

Additionally, we test whether Criterion 4.3 is independent of the diameters of the subdomains. For that purpose, we take square domains  $\Omega = [0, L]^2$ ,  $L = 1, 5, 10$ , of different sizes and choose  $k$  such that  $kL = 30$  is constant, i.e. such that the number of wavelengths in both coordinate directions in the squares of different sizes is constant, while the wave number varies. For all three cases, the DtN shows exactly the same behavior, that is reported in Table 2: the number of modes that are chosen and the number of iterations do not change with  $L$ . Criterion 4.3 consequently provides a useful strategy.

## 5. Sensitivity of the correction to the coarse space

In order to design and test a coarse space for the Helmholtz equation, it is indispensable to understand how it influences the eigenvalues of the preconditioned operator and hence the convergence behavior of the iterative method. For symmetric positive definite (s.p.d.) matrices, this question has been examined extensively e.g. in [39,40]. In particular, the coarse space does not make the effective condition number of the preconditioned matrix worse for any choice of  $Z$  [40, Theorem 2.1]. In this section, we examine to what extent these results apply to indefinite systems. We will see that contrarily to the s.p.d. case, for indefinite matrices there seems to be no way to ensure that using a two-level method with an arbitrarily chosen coarse space always accelerates the convergence. This is why choosing the right, problem dependent coarse space is important for indefinite systems as those arising from the Helmholtz equation.

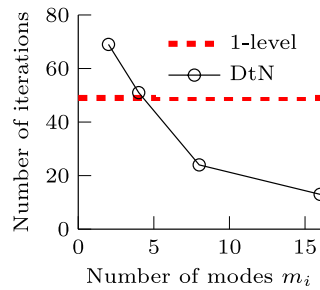


**Fig. 6.** Number of iterations in dependence of  $m_i$ . **Problem 2**,  $5 \times 5$  subdomains,  $n_{\text{loc}} = 40$ ,  $k = 29.3$ .

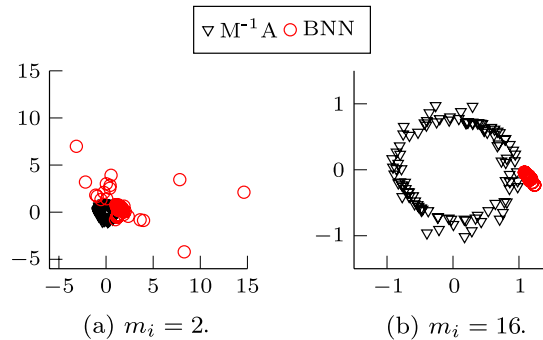


**Fig. 7.** 100 largest eigenvalues for  $M^{-1}A$  and BNN in the complex plane. **Problem 1**,  $5 \times 5$  subdomains,  $n_{\text{loc}} = 40$ ,  $k = 30$ .

### 5.1. Influence of the Dirichlet-to-Neumann coarse space on the spectrum

We compare the convergence rates and the spectrum of the two-level method (7) with DtN coarse space to those of the corresponding one-level RAS preconditioner (6). Apart from providing a more detailed understanding of our setting, these experiments can also be seen as a demonstration of the challenges that arise when designing a coarse space for an indefinite problem: Neither convergence rates nor the spectrum necessarily ameliorate when adding the second level even if it is carefully designed, c.f. [30].

Firstly, in Fig. 6, we compare the convergence rates of the one- and two-level methods for **Problem 2** from Section 6.2, using the setup described in Section 6.1. Note that in contrast to most of the other experiments, we do not choose **Problem 1** to make the problem simpler to solve with the one-level method (6). While using too few coarse space modes gives worse convergence rates than those of the one-level method, employing enough modes resolves the problem.

The next step is to look at the spectrum of the two operators for **Problem 1** from Section 6.2. We first motivate why it is reasonable to do this in the case of the GMRES method, which does not depend directly on the condition number as CG for s.p.d. matrices: The clustering of the eigenvalues is important for the convergence of the GMRES method [41]. As the eigenvalues for RAS all lie within a circle centered at the origin, we compare the largest eigenvalues without and with coarse space. If it decreases for the BNN preconditioner, the clustering is likely to be better. On the other hand, if it increases significantly, this is probably an indication for deterioration.

In Fig. 7, we compare the eigenvalue distribution of the one- and the two-level methods; the largest eigenvalues both of  $M^{-1}A$  and the BNN preconditioner are plotted in the complex plane. If the coarse space dimension is small, there is no clear structure in the eigenvalue distribution. While they lie within a circle of radius less than 1 with center  $(0, 0)$  for  $M^{-1}A$ , adding the coarse space with only a few modes has a chaotic effect, scattering the eigenvalues in the complex plane. This changes when adding more modes; the eigenvalues are then clustered near the point  $(1, 0)$ .

Consequently, choosing an incomplete or incorrect coarse space may have a detrimental effect both on convergence rates and on the spectrum. The coarse space has hence to be designed with the greatest care.

### 5.2. Understanding the effect of the coarse space for Hermitian matrices

In Section 5.1, we have shown that adding a second level to a preconditioner for an indefinite matrix may negatively affect both the convergence rates and the spectrum of the preconditioned operator. Here we give an explanation of this behavior and identify its causes. This is an extension of the results in [40] to indefinite systems. To be able to provide results, we restrict to a simpler setting: we assume that the matrix  $A$  is Hermitian which holds for the matrix associated to the Helmholtz problem defined in (5) if  $\Gamma_R = \emptyset$ . We examine deflation instead of the balancing preconditioner:



**Definition 5.1** (Deflation Operator). Let  $A \in \mathbb{C}^{n \times n}$  and let  $Z \in \mathbb{C}^{n \times r}$ ,  $r < n$ . If  $Z^*AZ$ ,  $*$   $\in \{T, \dagger\}$ , where  $T$  denotes the transpose and  $\dagger$  the conjugate transpose, is invertible, we define the deflation operator

$$P_D = I - A\mathcal{E}, \quad \text{where } \mathcal{E} = Z(Z^*AZ)^{-1}Z^*.$$

The deflation operator is closely related to the balancing preconditioner: If  $A = A^*$ , then  $P_{\text{BNN}}A$  and  $P_DA$  have the same eigenvalues except for those that are 0 and 1, respectively [39, Theorem 2.8]. In this section, we use Definition 5.1 with  $*$   $= \dagger$  the conjugate transpose.

Let  $v_i$ ,  $1 \leq i \leq n$  be an orthonormal basis of eigenvectors of  $A$  with corresponding eigenvalues  $\lambda_i \in \mathbb{R}$ . Let  $|\lambda_i| \leq |\lambda_{i+1}|$  for all  $1 \leq i < n$ . Let  $\lambda_{\min} = \min_{i: |\lambda_i| \neq 0} |\lambda_i|$ ,  $\lambda_{\max} = \max_i |\lambda_i|$ . We may consider the columns of  $Z$  separately in a recursive procedure, using a variant of [42, Theorem 3.2]:

**Theorem 5.2.** Let  $P^{(k)} = I - AZ_k(Z_k^\dagger AZ_k)^{-1}Z_k^\dagger$  with  $Z_k = [\tilde{Z}_1, \tilde{Z}_2, \dots, \tilde{Z}_k]$ , where  $\tilde{Z}_j \in \mathbb{C}^{n \times l_j}$  has full rank  $l_j$ . Let  $\tilde{Z}_i^\dagger \tilde{A}_{i-1} \tilde{Z}_i$  and  $Z_i^\dagger AZ_i$  be nonsingular for all  $1 \leq i \leq k$ . Then  $P^{(k)}A = P_k P_{k-1} \dots P_1 A$ , where  $P_{i+1} = I - \tilde{A}_i \tilde{Z}_{i+1} (\tilde{Z}_{i+1}^\dagger \tilde{A}_i \tilde{Z}_{i+1})^{-1} \tilde{Z}_{i+1}^\dagger$ ,  $\tilde{A}_i = P_i \tilde{A}_{i-1}$ ,  $\tilde{A}_0 = A$ .

The proof is literally the same for our situation. Hence we may restrict to  $Z \in \mathbb{C}^{n \times 1}$  with only one column,  $Z := \sum_{i \in I} \alpha_i v_i$ , where  $\alpha_i \in \mathbb{C}$  are coefficients and  $I \subseteq \{1, \dots, n\}$ . By computing  $P_D A v_k$  for all  $k$ , we get the following lemma:

**Lemma 5.3** (Structure of  $P_DA$ ). W.l.o.g. assume  $I = \{1, 2, \dots, |I|\}$ .  $P_DA$  in the basis of eigenvectors  $(v_i)_{1 \leq i \leq n}$  is a block diagonal matrix with the two blocks  $B$  and  $D$ , where  $B \in \mathbb{C}^{|I| \times |I|}$  is the block associated to  $(v_i)_{i \in I}$  and is defined by

$$B_{ii} = \frac{\sum_{k \neq i} |\alpha_k|^2 \lambda_i \lambda_k}{\sum_{k \in I} |\alpha_k|^2 \lambda_k}, \quad B_{ij} = -\frac{\alpha_j \bar{\alpha}_i \lambda_j \lambda_i}{\sum_{k \in I} |\alpha_k|^2 \lambda_k}, \quad \forall i, j \in I, i \neq j,$$

and  $D$  is a diagonal matrix with diagonal entries  $\lambda_{|I|+1}, \dots, \lambda_n$ .

The following theorem treats the simple cases in which bounds on the eigenvalues of the deflated operator can be guaranteed.

**Theorem 5.4.** If all  $\lambda_i$ ,  $i \in I$ , have the same sign, then

$$\lambda_{\max}(P_DA) \leq \lambda_{\max}(A) \quad \text{and} \quad \lambda_{\min}(P_DA) \geq \lambda_{\min}(A).$$

**Proof.** Let  $V$  be the matrix whose columns are the eigenvectors  $v_i$ ,  $1 \leq i \leq n$ . According to Lemma 5.3, after reordering,  $V^\dagger P_D A V$  has block structure with a block  $B$  associated to  $\{v_i\}_{i \in I}$  and a diagonal block  $D$ . As the two blocks are decoupled and all eigenvalues of  $D$  are eigenvalues of  $A$ , we can consider only  $B$ . As by assumption, all  $\lambda_i$ ,  $i \in I$ , have the same sign and eigenvalues are invariant under change of basis, either  $B$  or  $-B$  is Hermitian positive definite and we can use the result for the real, s.p.d. case [40, Theorem 2.1], whose proof is literally the same for complex matrices, to prove the claim.  $\square$

Theorem 5.4 shows that if all eigenvalues associated to the eigenvectors that contribute to the vector  $Z$  have the same sign, the spectrum of the deflated operator can be bounded by the one of the original operator. Deterioration of the spectrum could thus be avoided if an orthonormal basis of eigenvectors of the global operator was known. This is not feasible in practice.

The remaining question is what happens to the eigenvalues if the  $\lambda_i$ ,  $i \in I$ , have different signs. For simplicity, we restrict to the case  $|I| = 2$  and show that different signs of the eigenvalues do cause problems.

**Theorem 5.5.** Let  $|I| = 2$ , i.e.  $Z = \alpha_i v_i + \alpha_j v_j$  for some  $1 \leq i, j \leq n$ . Then we have  $\lambda_{\max}(P_DA) > \lambda_{\max}(A)$  if and only if  $i$  and  $j$  are chosen such that  $\lambda_i$  and  $\lambda_j$  have different signs and

$$\frac{(|\alpha_i|^2 + |\alpha_j|^2) |\lambda_i| |\lambda_j|}{|\alpha_i|^2 \lambda_i + |\alpha_j|^2 \lambda_j} > |\lambda_k| \quad \forall 1 \leq k \leq n. \quad (11)$$

**Proof.** This follows directly from Theorem 5.4 and Lemma 5.3, observing that the matrix  $B$  has the eigenvalues 0 and  $\frac{(|\alpha_i|^2 + |\alpha_j|^2) \lambda_i \lambda_j}{|\alpha_i|^2 \lambda_i + |\alpha_j|^2 \lambda_j}$ .  $\square$

Theorem 5.5 provides an explanation for the scattering of the eigenvalues observed in Fig. 7: if eigenvectors associated to eigenvalues with different signs enter the coarse space, the eigenvectors of the deflated matrix might grow arbitrarily large. However, the results are not able to explain the clustering of the eigenvalues that occurs when the coarse space dimension gets larger.

**Table 3**

Number of iterations (dimension of coarse space) for [Problem 1](#). Comparison of RAS method (6) without coarse space (1-level), and with DtN and PW ( $10^{-2}$ ) coarse spaces.

$n_{\text{loc}}$	$k$	5 × 5 subdomains				
		1-level	DtN	PW ( $10^{-2}$ )		
20	18.5	80	15	(144)	8	(352)
40	29.3	116	18	(224)	11	(467)
80	46.5	156	29	(299)	–	(577)
160	73.8	217	39	(508)	24	(609)

### 5.3. A modified deflation operator

In this section, we examine a variant of the deflation operator used e.g. in [\[23,27\]](#), where  $*$  =  $T$  in [Definition 5.1](#). Even though the transpose  $T$  seems to be more suitable for complex symmetric matrices than the conjugate transpose  $\dagger$ , as it is closely related to the structure of the matrix, we show that the situation with this choice is even worse.

We consider a complex symmetric, possibly non-Hermitian matrix  $A$  as it arises from the discretization of the Helmholtz equation (2). We assume that  $A$  is diagonalizable. It hence has an eigenvector matrix  $V$  such that  $V^T A V$  is diagonal and  $V^T V = I$  [[43](#), Theorem 4.4.13]. Under these assumptions, a modified version of [Theorem 5.5](#) holds, where Condition (11) is substituted by

$$\left| \frac{(\alpha_i^2 + \alpha_j^2) \lambda_i \lambda_j}{\alpha_i^2 \lambda_i + \alpha_j^2 \lambda_j} \right| > |\lambda_k| \quad \forall 1 \leq k \leq n.$$

Since the coefficients  $\alpha_i$  are complex numbers, the denominator  $|\alpha_i^2 \lambda_i + \alpha_j^2 \lambda_j|$  might become arbitrarily large independently of the signs of the eigenvalues. Hence, in contrast to the Hermitian case, no sign restriction on  $\lambda_i$  and  $\lambda_j$  can prevent the eigenvalues from becoming huge:

**Example 5.6.** Let  $A = \begin{pmatrix} 1 & i & 0 \\ i & 1 & 2i \\ 0 & 2i & 1 \end{pmatrix}$  with (orthogonal) eigenvectors  $v_1 = (1 \quad \sqrt{5} \quad 2)^T$ ,  $v_2 = (2 \quad 0 \quad -1)^T$ ,  $v_3 = (1 \quad -\sqrt{5} \quad 2)^T$  and eigenvalues  $\lambda_1 = 1 + i\sqrt{5}$ ,  $\lambda_2 = 1$ ,  $\lambda_3 = 1 - i\sqrt{5}$ . Choosing  $Z = \alpha \frac{1}{\|v_1\|} v_1 + \frac{1}{\|v_2\|} v_2$ ,  $\alpha = \sqrt{\frac{\varepsilon - \lambda_2}{\lambda_1}}$  for some real number  $0 < \varepsilon < 1$ , we get

$$\lambda_{\max}(P_D A) = \left| 1 + i\varepsilon^{-1}\sqrt{5} \right| > \lambda_{\max}(A) = \left| 1 + i\sqrt{5} \right|.$$

The theoretical results are clearly in favor of using the conjugate transpose. As the setting has been simplified in order to allow an easy investigation, we compare the matrices  $\mathcal{E}$  defined in [Definition 5.1](#) for  $*$   $\in \{T, \dagger\}$  used in the BNN method (7) with the DtN coarse space for the setting in [Table 3](#) with 5 × 5 subdomains. While the results for  $*$  =  $\dagger$  are shown in this table, the number of iterations for  $*$  =  $T$  are not reported because they are almost exactly the same and differ at most by 1. There hence seems to be almost no difference between the two operators. This result is different from [\[27, Section 4.1.2\]](#), where the authors conclude that the conjugate transpose outperforms the transpose, using however a different framework and example. We here choose the method using the conjugate transpose as it seems to be more robust. However, in contrast to the s.p.d. case, for none of the approaches an arbitrary choice of the coarse space  $W$  guarantees a gain compared to the one-level method, neither in terms of convergence rates nor in terms of bounds on the eigenvalues.

## 6. Numerical results

In this section, we examine the DtN coarse space numerically and compare it to the standard coarse space based on plane waves, c.f. [Section 1](#).

### 6.1. Framework and implementational details

We describe the framework in which the preconditioner (7) is used and give implementational details for the numerical experiments.

As a solver we use a generalized minimal residual (GMRES) method without restart using the BNN method (7) as a preconditioner. The termination criterion is based on the error  $\|u_h - u_i\|_\infty$ , where  $u_h$  is the exact finite element solution and  $u_i$  is the iterative solution in step  $i$ . The system is considered to be solved in step  $i$  if  $\frac{\|u_h - u_i\|_\infty}{\|u_h\|_\infty} < 10^{-7}$ . A bar “–” is used in the tables, when the maximum number of iterations, here 400, is reached. The initial iterate has pseudorandom values drawn from the standard uniform distribution on the interval (0, 1). The finite element part is implemented in FreeFem++ version 3.21 [[44](#)], and the algebraic part in MATLAB version 7.10.0.499 (R2010a).

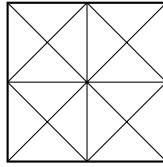


Fig. 8. Mesh.

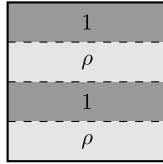


Fig. 9. Problem 1.

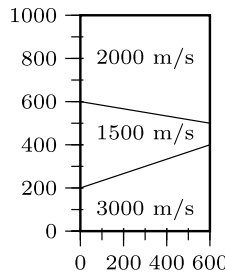


Fig. 10. Problem 3.

Due to the wave character of the solution, in all numerical experiments the grid has to be sufficiently fine in order for the discrete solution to be a good approximation of the continuous one. Additionally to the requirement of having a minimum number of points per wavelength, in order to avoid the *pollution effect* [2], not only  $kh$ , but also  $k^3h^2$  needs to be bounded from above. Various modifications, see e.g. [2] and references therein, of the finite element method are known to reduce this effect, but not considered here.

We choose an overlap  $L$  of two mesh elements as defined in Definition 3.1. If nothing else is specified a decomposition into  $N = n_S \times n_S$  squares is chosen. Let  $n_i$  be the number of grid points on one side of one square subdomain. If  $n_i = n_j$  for all  $1 \leq i, j \leq N$ , we define  $n_{loc} := n_i$ . In this case, the mesh is always of the type shown in Fig. 8. For decompositions using Metis [45], an arbitrary triangulation is chosen. We denote the number of grid points on one side of a square domain  $\Omega$  by  $n_{glob}$ .

## 6.2. Model problems

Here we define the model problems that are used in the numerical experiments in Sections 4–6. They are all based on the Helmholtz equation (2). The first example, Problem 1, c.f. [38], is the one that we investigate in most detail.

**Problem 1 (Open Cavity Problem).** In Eq. (2), let  $\Omega := [0, 1]^2$ ,  $\Gamma_D := \{0, 1\} \times [0, 1]$ , and  $\Gamma_R := [0, 1] \times \{0, 1\}$ . The right-hand side  $f$  is a point source at  $(0.5, 0.5)$ . The wave number  $k(\vec{x}) = \omega/c(\vec{x})$  is either constant, or the wave speed  $c$  is piecewise constant according to Fig. 9, where  $\rho \in \mathbb{R}$ ,  $\rho > 1$ .

**Problem 2 (Free Space Problem).** In Eq. (2), let  $\Omega := [0, 1]^2$ ,  $\Gamma_R := \partial\Omega$ , i.e. we simulate an unbounded region. The right-hand side  $f$  is a point source in the center  $(0.5, 0.5)$  of the domain  $\Omega$ . The wave number  $k$  is constant.

**Problem 3 (Wedge Problem).** This example mimics three layers with a simple heterogeneity. Let  $\Omega = (0, 600) \times (0, 1000)$   $m^2$  and  $\Gamma_R = \partial\Omega$  in Eq. (2). The right-hand side  $f$  is a point source located at  $(300, 980)$ . The wave number is given by  $k(\vec{x}) = \omega/c(\vec{x})$ , where  $c$  is defined in Fig. 10.

## 6.3. Plane waves

We introduce and shortly examine the coarse space based on plane waves. There is no consensus in the literature on how to define such a coarse space for different kinds of DDMs. We are in particular not aware of any work using plane waves in exactly our setting. Closest to our work are the methods presented in [25,46]. We use neither of these two approaches since,

as explained in Section 4.1, it is crucial that the homogeneous problems are solved locally in the interior of each subdomain, which is not the case in [25,46]. Our definition is based on numerical experiments and aims for good performance to have a serious competitor for the DtN coarse space; it might nevertheless be non-optimal.

A plane wave  $p^\theta : D \subset \mathbb{R}^d \rightarrow \mathbb{C}$  in direction  $\vec{\theta}$  is a function of the form

$$p^\theta(\vec{x}) = e^{i\bar{k}\theta\vec{x}}, \quad \vec{x} \in D, \quad \vec{\theta} \in \mathbb{R}^d, \quad \|\vec{\theta}\|_2 = 1. \quad (12)$$

Here  $\bar{k}$  is the mean value of the (possibly heterogeneous) wave number  $k$  on  $D$ . We proceed as in the case of the DtN operator, and modify Algorithm 4.1. We ignore Lines 1 and 2 and specify the functions  $\tilde{u}_i^k$  in Line 4 directly. Note that in contrast to DtN,  $m_i$  is chosen *a priori*. If nothing else is specified, we use  $m_i = 25$  modes per subdomain.

**Definition 6.1** (Plane Wave Coarse Space). Let  $1 \leq i \leq N$ . For each  $1 \leq k \leq m_i$  choose a direction  $\theta_k \in \mathbb{R}^d$ ,  $\|\theta_k\|_2 = 1$  and let  $\vec{g}_i^k \in \mathbb{C}^{n_{r_i}}$  be the coefficient vector of the finite element approximation of  $p^{\theta_k}$  defined in Eq. (12) on the interface  $\Gamma_i$ . Let  $\tilde{u}_i^k$  be the extension of  $\vec{g}_i^k$  in the sense of Definition 4.4.

It remains to be specified how the directions  $\theta_k$  are chosen. As in [24], we define them via a uniform discretization of the unit circle into circular sectors:

$$\theta_k := \begin{pmatrix} \cos(t_k) \\ \sin(t_k) \end{pmatrix}, \quad \text{where } t_k = \frac{2\pi(k-1)}{m_i}, \quad 1 \leq k \leq m_i.$$

The matrix  $Z$  based on plane waves can become rank deficient for a couple of reasons [24]. The rank deficiency of  $Z$  causes in the worst case divergence of the whole iterative scheme. To avoid this problem, we adapt the filtering of the coarse space described in [24], but apply filtering to functions defined on the entire subdomains instead of only the edges. We choose a filtering tolerance  $\epsilon$  and do the following: let  $Z$  have the blocks  $W_i$ . For each  $1 \leq i \leq N$ , perform the QR factorization of  $W_i$ , and then construct  $W_i^*$  as the union of the columns  $q_j$  of  $W_i$  for which  $|R_{jj}| > \epsilon$ . This is a local procedure that is performed on each subdomain separately. We substitute  $Z$  by the matrix constructed from the  $W_i^*$ . A too small value of  $\epsilon$  can cause the matrix  $Z$  to be still rank deficient. The authors of [24] propose to choose  $\epsilon$  rather too large than too small, setting  $\epsilon = 10^{-2}$ . We denote the method where the plane wave coarse space with filtering tolerance  $\epsilon$  is employed by PW( $\epsilon$ ).

As an adaptive strategy for choosing the coarse space size is crucial, we here examine to what extent it is provided by the filtering procedure. Therefore, we consider Problem 1 with  $n_{\text{loc}} = 40$ ,  $k = 29.3$  and a decomposition into  $5 \times 5$  subdomains. The dimension of the coarse space depends strongly on the number of modes per subdomain  $m_i$  that are initially chosen, even if the additional modes hardly influence the convergence rate: if we choose  $m_i = 16$ , the coarse space dimension is 384; with  $m_i = 32$  it is 459. However, the number of iterations is 13 versus 11 and hence did hardly change despite the larger, more expensive coarse space. Consequently, even though filtering provides some sort of adaptivity, it is sensitive to the number of modes that are initially chosen.

#### 6.4. Conditioning of coarse matrix

The condition number of the coarse matrix  $E = Z^\dagger AZ$  plays an important role. If it is too large, the iterative method might stagnate. Here we investigate to what extent the DtN coarse space suffers from conditioning problems.

The matrix  $Z$  is constructed from an orthonormal basis of eigenvectors defined on the interfaces of the subdomains. Their extensions to the interior of the subdomains are in general not orthogonal as the extension matrix  $A_{\Gamma}^{-1}A_{I\Gamma}$  is not unitary and hence does not conserve orthogonality. Nevertheless, in the numerical experiments for Problem 1 the condition number for DtN behaves well: in Fig. 11(a), we examine the dependence of the condition number on the coarse space size and compare it to the one for plane waves, with and without filtering. For the DtN, the condition number of  $E$  is only mildly affected by the coarse space dimension. The same is true for plane waves with filtering, but here the upper bound is significantly larger. In Fig. 11(b), we investigate whether this behavior carries over to a broader range of wave numbers  $k$ . We choose a fixed number  $m_i = 16$  of modes per subdomain. If  $k$  and  $h$  are varied such that  $k^3h^2$  is constant, the condition number for DtN remains almost constant. So filtering of the coarse modes is not necessary here. Furthermore, the condition number is significantly lower than for the plane waves.

#### 6.5. Performance for homogeneous open cavity problem

We study the performance of the DtN coarse space for Problem 1 with homogeneous wave number. In Table 3, the number of iterations for different  $k$  is shown. It increases slightly with  $k$  if  $k^3h^2$  is constant. This could be due to the decreasing physical size  $Lh$  of the overlap, c.f. Table 6. Moreover, the dimension of the DtN coarse space depends linearly on the wave number  $k$ . We also show the results for PW ( $10^{-2}$ ) and see the effect the ill-conditioning of the plane wave coarse matrix  $Z$  has: for  $k = 46.5$ , the method with the plane wave coarse space stagnates at a certain error and thus never reaches the desired tolerance, even though filtering is employed. This problem could be cured with a different filtering tolerance  $\epsilon$  or number of modes  $m_i$ . However, we are not aware of any strategy that reliably chooses these parameters *a priori* for a general example.

In Table 3 we have seen that the number of iterations is smaller with the PW than with the DtN coarse space. However, it is not fair to compare these numbers as the dimensions of the coarse spaces differ significantly. Therefore, in Table 4 we

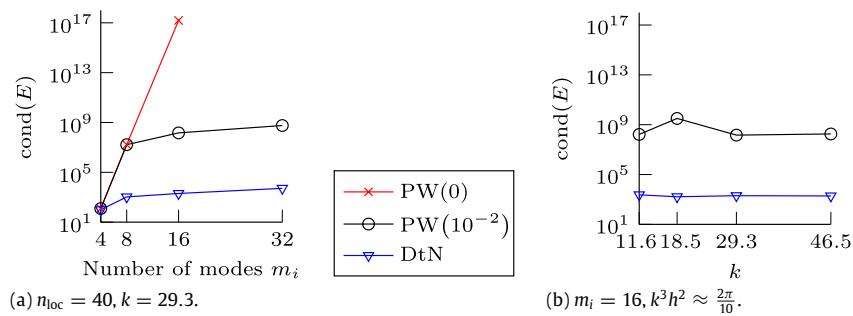


**Fig. 11.** Condition number of coarse matrix  $E$ . Problem 1,  $5 \times 5$  subdomains.

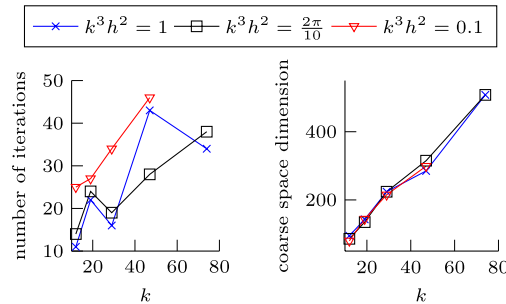


**Fig. 12.** Testing different values of  $k^3 h^2$ . Problem 1,  $5 \times 5$  subdomains.

**Table 4**

Comparison of number of iterations with identical coarse space size for DtN and PW ( $10^{-2}$ ).  $5 \times 5$  subdomains, Problem 1.

$n_{\text{loc}}$	$k$	$m_i$ from DtN coarse space			$m_i$ from PW coarse space		
		$m_i$	DtN	PW ( $10^{-2}$ )	$m_i$	DtN	PW ( $10^{-2}$ )
10	11.6	4	14	17	12	8	7
20	18.5	6	21	23	15	9	9
40	29.3	9	23	22	17	13	12
80	46.5	12	35	35	24	18	16
160	73.8	21	38	29	25	36	24

**Table 5**

Dependence of number of iterations (coarse space dimension) on wave number for fixed mesh width. Problem 1,  $5 \times 5$  subdomains,  $n_{\text{loc}} = 120$ .

$k$	1-level	DtN
5	106	88 (25)
10	115	68 (70)
15	117	61 (90)
30	133	31 (224)
45	169	36 (299)

compare the two methods forcing the dimension to be the same by prescribing a fixed number of modes  $m_i$  on each subdomain also for DtN. These numbers  $m_i$  are the same on all subdomains and are computed by dividing the sizes in Table 3 by the number of subdomains. With this setting, DtN and PW yield approximately the same convergence rates. We note that for  $k = 46.5$ , choosing  $m_i = 24$  instead of  $m_i = 25$  solves the problem of stagnating convergence observed for the corresponding test in Table 3. Consequently, the PW method is sensitive to the slightest change in the parameters.

In Fig. 12, we examine whether the convergence rates depend on the value of the constant  $k^3 h^2$ . There is no clear indication which value might be optimal, but a rather fine grid gives the highest number of iterations absolutely. The coarse space dimension depends on  $k$  but is independent of the grid width.

In Table 5, the mesh width is kept fixed and the wave number is varied. We see how the coarse space dimensions increases with  $k$ . The number of iterations remains only constant if  $k$  is large enough. For  $k$  small, the coarse space built with Criterion 4.3 is so small that the number of iterations remains rather large.

**Table 6**Dependence of number of iterations (coarse space dimension) on overlap/mesh width. Problem 1,  $5 \times 5$  subdomains.

$k$	$n_{loc} = 20, L = 2$			$n_{loc} = 80, L = 2$			$n_{loc} = 80, L = 8$		
	1-level	DtN		1-level	DtN		1-level	DtN	
1	73	56	(25)	94	81	(25)	66	39	(25)
5	64	43	(25)	96	78	(25)	55	37	(25)
10	68	21	(74)	106	49	(74)	66	22	(74)
20	84	32	(139)	107	32	(144)	86	33	(139)

**Table 7**

Dependence of number of iterations (coarse space dimension) on number of subdomains. DtN coarse space, Problem 1.

$n_{loc}$	$k$	Number of subdomains							
		$5 \times 5$		$5 \times 10$		$5 \times 20$		$5 \times 40$	
10	11.6	15	(80)	18	(160)	22	(320)	30	(640)
20	18.5	15	(144)	15	(314)	16	(654)	19	(1334)
40	29.3	18	(224)	18	(484)	20	(1004)	22	(2044)
80	46.5	29	(299)	37	(624)	48	(1274)	66	(2574)

**Table 8**Second scaling test: We keep the problem fixed but vary the number of subdomains. We give the number of iterations (it.), the dimension of the coarse system (size) and the time needed to solve the algebraic equations (time). The global number of grid points in each direction is 320, the wave number  $k = 40$ . We decompose  $\Omega = [0, 1]^2$  uniformly into squares.

# Subdomains	DtN			PW ( $10^{-2}$ )		
	# it.	Size	Time (s)	# it.	Size	Time (s)
$2 \times 2$	23	(68)	2.90e2	17	(96)	3.08e2
$4 \times 4$	35	(200)	2.67e2	16	(368)	2.71e2
$8 \times 8$	44	(416)	1.80e2	12	(1116)	5.76e2
$16 \times 16$	57	(960)	4.78e2	10	(3256)	3.97e3
$32 \times 32$	47	(2944)	3.72e3	8	(9208)	3.28e4

In Table 6, two properties of the DtN coarse space and of Criterion 4.3 become visible: On the one hand, for small  $k$ , only one mode per subdomain is chosen and the number of iterations is hardly influenced by the coarse space. This is not a flaw of the coarse space itself, but due to Criterion 4.3; choosing more modes results in a stronger impact on convergence rates. For the homogeneous case this is not a problem as cases with very small wave number  $k$  can be solved by standard methods.

On the other hand, we study the influence of mesh refinement. If the mesh is refined twice and the overlap stays constant in terms of number of elements  $L$ , see the central columns of Table 6, the convergence rates deteriorate a lot; in the worst cases we get more than a factor 2 more iterations with about the same coarse space size. If however  $Lh$ , i.e. the physical size of the overlap, is constant, see the last three columns of Table 6, the number of iterations even decreases if the mesh is refined. This behavior is probably due to the transmission conditions that make the convergence rates depend on the size of the overlap [38]. Within this context, it might be worth to investigate more advanced transmission conditions, e.g. optimized ones [34].

In Table 7, we vary the number of subdomains in one direction and keep the number of wavelengths per subdomain fixed. The coarse space dimension grows approximately linearly with the number of subdomains as expected from the construction. Unfortunately, the increase in the coarse space dimension is insufficient to keep the iteration numbers constant if the number of wavelength in the global domain grows. This might at least partially be due to the fact that the transmission conditions that we employ are non-optimal.

In Table 8, we perform a similar test. In contrast to the previous experiment, we now keep the number of wavelengths in the global domain fixed and only vary the number of subdomains in both directions. Here, the iteration numbers increase slightly even though a larger and larger coarse space is chosen. For the PW coarse space on the other hand, the resulting coarse space is not only significantly larger, up to a factor of  $>3$  than the DtN one but also grows at a higher rate. For the case of  $32 \times 32$ , the number of degrees of freedom amounts to roughly 9% of the unknowns for the one-level method. This even causes the iteration numbers to decrease with respect to the case of fewer subdomain. However, each assembly of the coarse matrix and each iteration step are very costly as the coarse system has a block structure with overlapping, fully populated blocks, and data needs to be gathered/scattered from/to all subdomains. This can also be seen in the timings that we additionally give in Table 8. Even though our implementation is serial and not optimized, the detrimental effect in time to solution of the large coarse system can be seen especially for the  $32 \times 32$  subdomains case.

Summarizing, the PW coarse space suffers from conditioning problems and there is no strategy on how to choose the parameters involved. The construction of the DtN coarse space resolves these issues, providing a reliable criterion on which



modes to choose. For the homogeneous test cases, the performance of the DtN in terms of iteration numbers is not better than that of PW. In fact, iteration numbers in almost all tables are better for the latter as the coarse space dimension for PW is significantly larger with the parameters that we have chosen. The comparison in Table 4 however shows that in case the coarse space dimension is the same for both examples, they deliver comparable performance. The advantage of our approach in this case hence lies in the easier usability and the reliability. Despite the more expensive construction, the DtN coarse space might even be more efficient in total, as for PW choosing the wrong parameters can easily lead to a coarse space that is significantly larger than necessary.

#### 6.6. Performance for heterogeneous open cavity problem

In this section, we study some small heterogeneous test cases for Problem 1. In Table 9, the iteration numbers for constant  $k^3 h^2$  are shown. For PW, for some cases convergence stagnated due to ill-conditioning despite the rather large filtering tolerance. Moreover, the adaptively chosen coarse space size for DtN is significantly smaller than that for PW. This also has a small effect on the convergence rates, with PW performing better. As in the homogeneous case, the coarse space size increases with the wave number.

In Table 10, we vary the contrast  $\rho := k_{\max}/k_{\min}$ . With increasing contrast, the convergence rates for the one-level method deteriorate. For DtN, even though the coarse space size decreases, the number of iterations grows only slightly. Only for larger contrast, the situation deteriorates. In the parts of the domain where  $\rho$  is large, the problem is very close to the Laplacian and hence almost positive definite. As we have seen in Table 6, DtN does not work well for such situations since the coarse space is too small to enhance convergence. PW does not suffer from this problem, because the coarse space size is not chosen adaptively. Here again the ill-conditioning prevents the PW method from convergence; we therefore also provide the results with an adapted filtering tolerance of  $10^{-1}$ .

We now choose the same coarse space dimension for both DtN and PW, see Table 11, to verify that the better convergence rates for PW are due to the size of the coarse space. In contrast to the homogeneous case in Table 4, for the heterogeneous one DtN performs significantly better than PW when the number of modes chosen is the same, in particular for larger wave numbers.

Concluding, we note that the conditioning difficulties for PW detected in Section 6.5 seem to be even more serious for the heterogeneous examples. Moreover, for the heterogeneous case, we have seen in Table 11, that the DtN approach indeed provides better results if the coarse space dimension is the same.

#### 6.7. Extension to other problems

In this section, we consider also the other examples defined in Section 6.2 to confirm that our results are valid for a broader range of examples.

*Irregular decomposition.* In all the previous experiments, we have used a decomposition into square subdomains to ensure reproducibility. Here we show that this restriction is not necessary for the method to work. In Table 12 we consider Problem 1, where both the decomposition done with Metis [45] and the triangulation are now irregular. Compared to the regular case in Table 3, the method behaves similarly. While the dimension of the coarse space increases slightly, the number of iterations is almost the same.

*Free space problem.* Here we examine Problem 2, where non-reflecting boundary conditions are imposed on the entire boundary. The iteration numbers for different partitions are reported in Table 13. The qualitative behavior is similar to the one observed for Problem 1 in Table 3, but the absolute number of iterations is lower, in particular for the one-level method.

*Wedge problem.* As a last example, we consider the wedge problem, Problem 3. The results are reported in Table 14. Also for this case, the 2-level method with the coarse space based on the DtN operator shows a good behavior. To be able to compare with the results for the unit square, note that the number of wave-lengths in the  $y$ -direction for the smallest angular frequency  $\omega = 90$  corresponds to a wave number  $k$  varying between 30 and 60 for the unit square.

## 7. Conclusions

We have introduced and tested a two-level domain decomposition method for an efficient solution of the heterogeneous Helmholtz equation discretized with piecewise linear finite elements. The important new ingredient is the coarse space. Its construction is based on local eigenproblems involving the Dirichlet-to-Neumann operator and can be performed efficiently in parallel. The resulting method has been tested successfully on 2D model problems and compared to the standard approach with a coarse space based on plane waves. The extension to 3D problems is straightforward.

The construction of the DtN coarse space inherently respects variations in the wave number, making it possible to treat heterogeneous Helmholtz problems. Moreover, it does not suffer from ill-conditioning as the standard approach based on plane waves, even if many coarse modes are chosen. This is an important property as ill-conditioning can cause the iterative method to stagnate.

Our construction is based on local eigenvalue problems which are more costly than an explicit plane wave coarse space. However, the solution of these eigenvalue problems can be performed in parallel and should not affect the scalability of the

**Table 9**

Number of iterations (coarse space dimension). Heterogeneous [Problem 1](#),  $5 \times 5$  subdomains.

$n_{\text{loc}}$	$\omega$	$\rho = 5$				$\rho = 10$			
		DtN		PW ( $10^{-2}$ )		DtN		PW ( $10^{-2}$ )	
10	11.6	18	(69)	8	(229)	19	(69)	8	(214)
20	18.5	23	(111)	10	(274)	23	(111)	11	(263)
40	29.3	31	(159)	13	(339)	35	(159)	16	(326)
80	46.5	33	(242)	–	(442)	40	(236)	–	(414)
160	73.8	47	(388)	–	(519)	57	(378)	42	(494)

**Table 10**

Varying contrast. Number of iterations (coarse space dimension) for heterogeneous [Problem 1](#),  $5 \times 5$  subdomains,  $n_{\text{loc}} = 80$ ,  $\omega = 46.5$ .

$\rho$	1-level	DtN		PW ( $10^{-2}$ )		PW ( $10^{-1}$ )	
$10^0$	156	29	(299)	43	(577)	16	(505)
$10^1$	154	40	(236)	–	(414)	26	(346)
$10^2$	173	52	(236)	–	(388)	33	(320)
$10^3$	177	53	(236)	–	(379)	35	(315)

**Table 11**

Fixed coarse space size. Number of iterations (coarse space dimension) for heterogeneous [Problem 1](#),  $\rho = 10$ ,  $5 \times 5$  subdomains.

$n_{\text{loc}}$	$\omega$	$m_i$	DtN		PW ( $10^{-2}$ )	
10	11.6	3	18	20	(75)	
20	18.5	5	20	24	(123)	
40	29.3	7	31	40	(171)	
80	46.5	10	38	55	(237)	
160	73.8	16	57	89	(356)	

**Table 12**

Number of iterations (coarse space dimension) for homogeneous [Problem 1](#). 25 subdomains with Metis [45].

$n_{\text{glob}}$	$k$	1-level	DtN	
50	11.6	64	14	(116)
100	18.5	92	15	(168)
200	29.3	130	20	(257)
400	46.5	173	29	(381)
800	73.8	256	36	(645)

**Table 13**

Number of iterations (coarse space dimension) for [Problem 2](#).

$k$	$n_{\text{glob}}$	$5 \times 5$ subdomains				$10 \times 10$ subdomains			
		DtN		PW ( $10^{-2}$ )		DtN		PW ( $10^{-2}$ )	
18.5	100	15	(144)	8	(355)	16	(364)	7	(1152)
29.3	200	18	(224)	11	(466)	22	(460)	9	(1288)
46.5	400	26	(315)	–	(577)	43	(660)	12	(1712)
73.8	800	30	(514)	24	(609)	47	(956)	16	(2346)

**Table 14**

Number of iterations (coarse space dimension). [Problem 3](#) decomposed with Metis.

$\omega$	$n$	$15$ subdomains				$60$ subdomains			
		DtN		PW ( $10^{-2}$ )		DtN		PW ( $10^{-2}$ )	
90	$150 \times 250$	14	(267)	13	(346)	22	(541)	11	(1038)
180	$300 \times 500$	16	(514)	33	(375)	23	(1074)	22	(1426)
360	$600 \times 1000$	20	(968)	73	(375)	25	(2113)	86	(1500)

algorithm. In contrast to the plane wave based coarse space, where several parameters need to be adapted carefully to the problem under consideration, our completely automatic construction refrains from the need of parameter tuning.

Our analysis has shown that linear combinations of eigenvectors associated to eigenvalues with different signs that enter the coarse space cause problems if the coarse space is incomplete, possibly making convergence rates worse than those of

the one-level method. Our mode selection criterion ensures that all important modes are present, hence guaranteeing good convergence rates.

## References

- [1] A. Moiola, E.A. Spence, Is the Helmholtz equation really sign-indefinite? 2012, Preprint.
- [2] I.M. Babuška, S.A. Sauter, Is the pollution effect of the FEM avoidable for the Helmholtz equation considering high wave numbers? *SIAM Rev.* 42 (2000) 451–484.
- [3] O.G. Ernst, M.J. Gander, Why it is difficult to solve Helmholtz problems with classical iterative methods, in: I. Graham, T. Hou, O. Lakkis, R. Scheichl (Eds.), *Numerical Analysis of Multiscale Problems*, in: *Lecture Notes in Computational Science and Engineering*, vol. 83, Springer, Berlin, Heidelberg, 2012, pp. 325–363.
- [4] Y.A. Erlangga, Advances in iterative methods and preconditioners for the Helmholtz equation, *Arch. Comput. Methods Eng.* 15 (2008) 37–66.
- [5] M. Magolu Monga Made, Incomplete factorization-based preconditionings for solving the Helmholtz equation, *Internat. J. Numer. Methods Engrg.* 50 (2001) 1077–1101.
- [6] D. Osei-Kuffuor, Y. Saad, Preconditioning Helmholtz linear systems, *Appl. Numer. Math.* 60 (2010) 420–431.
- [7] M. Bollhöfer, M.J. Grote, O. Schenk, Algebraic multilevel preconditioner for the Helmholtz equation in heterogeneous media, *SIAM J. Sci. Comput.* 31 (2009) 3781–3805.
- [8] M.J. Gander, F. Nataf, AILU for Helmholtz problems: a new preconditioner based on the analytic parabolic factorization, *J. Comput. Acoust.* 9 (2001) 1499–1506.
- [9] B. Engquist, L. Ying, Sweeping preconditioner for the Helmholtz equation: hierarchical matrix representation, *Comm. Pure Appl. Math.* 64 (2011) 697–735.
- [10] A. Bayliss, C.I. Goldstein, E. Turkel, An iterative method for the Helmholtz equation, *J. Comput. Phys.* 49 (1983) 443–457.
- [11] Y.A. Erlangga, C. Vuik, C.W. Oosterlee, On a class of preconditioners for solving the Helmholtz equation, *Appl. Numer. Math.* 50 (2004) 409–425.
- [12] A. Brandt, I. Livshits, Wave-ray multigrid method for standing wave equations, *Electron. Trans. Numer. Anal.* 6 (1997) 91.
- [13] H.C. Elman, O.G. Ernst, D.P. O’Leary, A multigrid method enhanced by Krylov subspace iteration for discrete Helmholtz equations, *SIAM J. Sci. Comput.* 23 (2002) 1291–1315.
- [14] A. Toselli, O.B. Widlund, *Domain Decomposition Methods—Algorithms and Theory*, Springer-Verlag, 2005.
- [15] M.J. Gander, H. Zhang, Domain decomposition methods for the Helmholtz equation: a numerical investigation, in: *Domain Decomposition Methods in Science and Engineering XX*, in: *Lecture Notes in Computational Science and Engineering*, Springer, San Diego, 2012.
- [16] B. Després, *Méthodes de décomposition de domaine pour les problèmes de propagation d’ondes en régime harmonique*, Ph.D. Thesis, Université de Paris IX, Dauphine, Paris, 1991.
- [17] A. Toselli, Some Results on Overlapping Schwarz Methods for the Helmholtz Equation Employing Perfectly Matched Layers, Technical Report 765, Courant Institute of Mathematical Sciences, New York University, New York, 1998.
- [18] A. Schädle, L. Zschiedrich, Additive Schwarz method for scattering problems using the PML method at interfaces, in: *Domain Decomposition Methods in Science and Engineering XVI*, 2007, pp. 205–212.
- [19] C.C. Stolk, A rapidly converging domain decomposition method for the Helmholtz equation, *J. Comput. Phys.* 241 (2013) 240–252.
- [20] F. Collino, S. Ghanemi, P. Joly, Domain decomposition method for harmonic wave propagation: a general presentation, *Comput. Methods Appl. Mech. Engrg.* 184 (2000) 171–211.
- [21] M.J. Gander, F. Magoulès, F. Nataf, Optimized Schwarz methods without overlap for the Helmholtz equation, *SIAM J. Sci. Comput.* 24 (2002) 38–60.
- [22] Y. Boubendir, X. Antoine, C. Geuzaine, A quasi-optimal non-overlapping domain decomposition algorithm for the Helmholtz equation, *J. Comput. Phys.* 231 (2012) 262–280.
- [23] C. Farhat, A. Macedo, M. Lesoinne, A two-level domain decomposition method for the iterative solution of high frequency exterior Helmholtz problems, *Numer. Math.* 85 (2000) 283–308.
- [24] C. Farhat, P. Avery, R. Tezaur, L. Jing, FETI-DPH: a dual-primal domain decomposition method for acoustic scattering, *J. Comput. Acoust.* 13 (2005) 499–524.
- [25] J.-H. Kimn, M. Sarkis, Restricted overlapping balancing domain decomposition methods and restricted coarse problems for the Helmholtz problem, *Comput. Methods Appl. Mech. Engrg.* 196 (2007) 1507–1514.
- [26] J. Li, X. Tu, Convergence analysis of a balancing domain decomposition method for solving a class of indefinite linear systems, *Numer. Linear Algebra Appl.* 16 (2009) 745–773.
- [27] R. Aubry, S. Dey, R. Löhner, Iterative solution applied to the Helmholtz equation: complex deflation on unstructured grids, *Comput. Methods Appl. Mech. Engrg.* (2012).
- [28] V. Dolean, F. Nataf, R. Scheichl, N. Spillane, Analysis of a two-level Schwarz method with coarse spaces based on local Dirichlet-to-Neumann maps, *Comput. Methods Appl. Math.* 12 (2012) 391–414.
- [29] F. Nataf, H. Xiang, V. Dolean, N. Spillane, A coarse space construction based on local Dirichlet-to-Neumann maps, *SIAM J. Sci. Comput.* 33 (2011) 1623–1642.
- [30] J. Fish, Y. Qu, Global-basis two-level method for indefinite systems. Part 1: convergence studies, *Internat. J. Numer. Methods Engrg.* 49 (2000) 439–460.
- [31] D. Givoli, High-order local non-reflecting boundary conditions: a review, *Wave Motion* 39 (2004) 319–326.
- [32] F. Ihlenburg, *Finite Element Analysis of Acoustic Scattering*, Vol. 132, Springer, 1998.
- [33] X.-C. Cai, M.A. Casarin, F.W. Elliott Jr., O.B. Widlund, Overlapping Schwarz algorithms for solving Helmholtz’s equation, *Contemp. Math.* 218 (1998) 391–399.
- [34] M.J. Gander, Optimized Schwarz methods, *SIAM J. Numer. Anal.* 44 (2006) 699–731.
- [35] J. Mandel, Balancing domain decomposition, *Comm. Numer. Methods Engrg.* 9 (1993) 233–241.
- [36] Y.A. Erlangga, R. Nabben, Deflation and balancing preconditioners for Krylov subspace methods applied to nonsymmetric matrices, *SIAM J. Matrix Anal. Appl.* 30 (2008) 684–699.
- [37] J. Galvis, Y. Efendiev, Domain decomposition preconditioners for multiscale flows in high-contrast media, *Multiscale Model. Simul.* 8 (2010) 1461–1483.
- [38] M.J. Gander, L. Halpern, F. Magoulès, An optimized Schwarz method with two-sided Robin transmission conditions for the Helmholtz equation, *Internat. J. Numer. Methods Fluids* 55 (2007) 163–175.
- [39] R. Nabben, C. Vuik, A comparison of deflation and the balancing preconditioner, *SIAM J. Sci. Comput.* 27 (2006) 1742–1759.
- [40] R. Nabben, J.J. Tang, C. Vuik, Deflation acceleration for domain decomposition preconditioners, in: P.H.P. Wesseling, C.W. Oosterlee (Eds.), *Proceedings of the 8th European Multigrid Conference*, Scheveningen, The Hague, The Netherlands, Delft, September 27–30, 2005.
- [41] Y. Saad, M.H. Schultz, GMRES: a generalized minimal residual algorithm for solving nonsymmetric linear systems, *SIAM J. Sci. Stat. Comput.* 7 (1986) 856–869.
- [42] T.B. Jönsthövel, M.B. Van Gijzen, C. Vuik, A. Scarpas, On the use of rigid body modes in the deflated preconditioned conjugate gradient method, *SIAM J. Sci. Comput.* 35 (2013) B207–B225.
- [43] R.A. Horn, C.R. Johnson, *Matrix Analysis*, Cambridge University Press, 1990.
- [44] F. Hecht, O. Pironneau, A. Le Hyaric, K. Ohtsuka, FreeFem++, Université Pierre et Marie Curie, 2007. <http://www.freefem.org/ff++/ftp/freefem++doc.pdf>.
- [45] G. Karypis, V. Kumar, A fast and high quality multilevel scheme for partitioning irregular graphs, *SIAM J. Sci. Comput.* 20 (1998) 359–392.
- [46] A. Leong, Extension of two-level Schwarz preconditioners to symmetric indefinite problems, Master’s Thesis, New York University, Courant Institute of Mathematical Sciences, 2008.